

## Condensation in Disordered Lasers: Theory, 3D + 1 Simulations, and Experiments

C. Conti,<sup>1</sup> M. Leonetti,<sup>2</sup> A. Fratolocchi,<sup>3,1</sup> L. Angelani,<sup>4</sup> and G. Ruocco<sup>1,2</sup>

<sup>1</sup>Research Center Soft INFM-CNR, c/o Università di Roma "Sapienza," I-00185, Roma, Italy

<sup>2</sup>Dipartimento di Fisica, Università di Roma "Sapienza," I-00185, Roma, Italy

<sup>3</sup>Centro Studi e Ricerche "Enrico Fermi," Via Panisperna 89/A, I-00184, Roma, Italy

<sup>4</sup>Research Center SMC INFM-CNR, c/o Università di Roma "Sapienza," I-00185, Roma, Italy

(Received 30 May 2008; published 30 September 2008)

The complex processes underlying the generation of a coherent emission from the multiple scattering of photons and wave localization in the presence of structural disorder are still mostly unexplored. Here we show that a single nonlinear Schrödinger equation, playing the role of the Schwalow-Townes law for standard lasers, quantitatively reproduces experimental results and three-dimensional time-domain parallel simulations of a colloidal laser system.

DOI: 10.1103/PhysRevLett.101.143901

PACS numbers: 42.55.Zz, 42.65.Sf, 67.85.Bc

Random lasers (RL) are a rapidly growing field of research, with implications in soft-matter physics, light localization, and photonic devices [1,2]. Since the pioneering investigations [3,4], different groups reported on experimental observations, from paint pigments to human tissue [5–9]. In all of these cases a coherentlike narrow spectral line emerges from the fluorescence as the pump energy is increased, and, in some instances, several spectral peaks have been reported [9,10].

In standard single-mode lasers, without structural disorder, the emission linewidth is linked to the electromagnetic energy stored in the cavity by the so-called Schwalow-Townes (ST) law [11,12]. An equivalent law for RL is missing. Nevertheless, various issues (such as the statistical properties and the link with spin-glass theory [9,13–17]) were theoretically analyzed, while the leading model (quantitatively compared with experiments) is that based on the light-diffusion approximation [18–21], which, however, overlooks the ondulatory character of the involved photons. Within a different perspective, RL are due to several localized electromagnetic (EM) states put into oscillations in a disordered environment (as, e.g., in [9,17,22,23]). In this framework, it is expected that the number of involved modes increases with the pump energy and, correspondingly, the spectrum widens. However, exactly the opposite happens, and this is also accompanied by the shortening of the emitted pulse [24–26]. In addition, the fact that strong (or Anderson) localization of light sustains the RL action is still debated. *Ab initio* computational studies were limited to 1D and 2D geometries [27,28], not accounting for the critical character of three-dimensional (3D) localization [29]. Monte Carlo simulations neglect interference effects [30–32].

Here we report on an original theoretical formulation; we quantitatively compare its predictions with experiments and with the first ever reported 3D + 1 *ab initio* Maxwell-Bloch simulations. We show that the RL linewidth is ruled

by a nonlinear differential equation, which is the equivalent of the ST law, and is formally identical to the nonlinear Schrödinger, or Gross-Pitaevskii (GP), equation governing ultracold atoms [33]. There is hence a strict connection between photons in RL and ultracold bosons; the spectral narrowing observed in RL is thus ascribed to a *condensation process* [34] of the involved electromagnetic resonances.

*Simulations.*—We consider a vectorial formulation of the Maxwell-Bloch equations [35,36]. 21 nonlinear stochastic partial differential equations are solved by finite-difference time-domain (FDTD) discretization on a grid distributed on (typically) 256 processors. We model an active medium that is infiltrated in the voids of a granular distribution of particles obtained by molecular dynamics [37]. We consider 8000 TiO<sub>2</sub> particles (average diameter 300 nm) with refractive index 2.9 (Fig. 1). The gain bandwidth is 230 nm ( $\sim 1/t_g$ , with  $t_g$  the lifetime), and the central wavelength is  $\lambda_0 = 590$  nm ( $\omega_0$  is the angular frequency). Amplification is only present in the interstices between colloidal spheres with the pump rate (varied by the atomic inversion density  $N_a$ ; see [35,36]) constant over the  $\sim 3$  ps simulation. The lasing action is self-starting from the noise due spontaneous emission modeled as a stochastic term.

In the absence of light amplification, the response to a single cycle pulse ( $\sim 1$  fs) at wavelength  $\lambda = 532$  nm (Fig. 1) unveils several spectral peaks corresponding to long-living modes. Field spatial distribution (inset in Fig. 1) is determined by continuous-wave excitation.

Then we simulate the RL action: When increasing the pumping, a coherent field is built from noise. Figure 2(a) shows the snapshot of the EM energy density in the sample middle section. In Figs. 2(b) and 2(c), we display the spectra for two pumping levels in quantitative agreement with the experiments below. The 3D-RL action is mediated by several modes with overlapping resonances. In real-

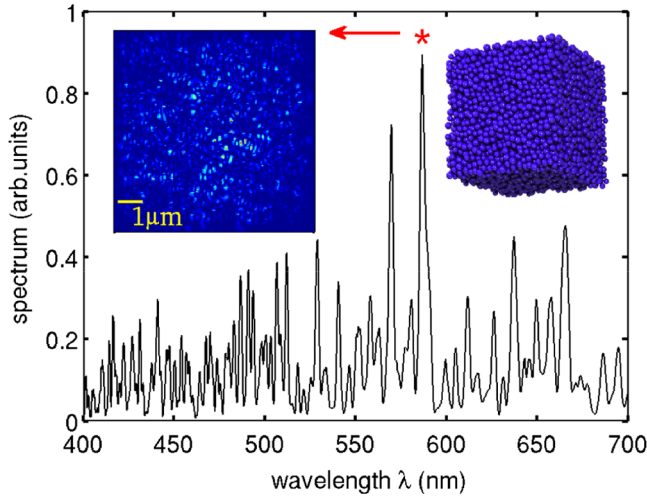


FIG. 1 (color online). Electromagnetic spectrum as obtained after a wideband excitation; the left inset shows the energy density in the middle section ( $\lambda = 586.5$  nm, asterisk); a sketch of the system is also shown on the right.

world samples, the RL volume and the number of modes  $N$  are much larger than those found in our simulations; the outcome is a smoother emission profile (Fig. 4).

*Gross-Pitaevskii equation.*—The RL frequency content is given by  $A(\omega)$ , such that  $|A(\omega)|^2$  is the energy stored in the disordered cavity at relative angular frequency  $\omega$  with respect to  $\omega_0$ . The loss coefficient is  $\alpha(\omega)$ , and the gain  $g$  depends on the whole shape  $A(\omega)$ , as due to the nonlinear susceptibility of the resonant medium [17]. In the frequency domain, the oscillation condition “gain = loss” reads as  $g[A(\omega)] = \alpha(\omega)A(\omega)$ . Limiting for the moment to the loss profile  $\alpha(\omega)$ , and following the previous numerical analysis, one has that, in a disordered system sustaining various resonances,  $\alpha(\omega)$  is a smooth function interleaved by narrow spectral dips, corresponding to  $N$  localized (high- $Q$  factor) long-living modes (see Fig. 1).

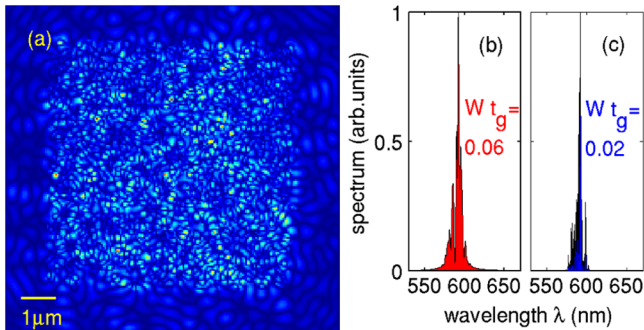


FIG. 2 (color online). 3D + 1 Maxwell-Bloch simulation of RL: (a) energy distribution in the sample middle section; (b) spectrum for  $N_a = 2 \times 10^{24} \text{ m}^{-3}$ ; (c) as in (b) for  $N_a = 5 \times 10^{24} \text{ m}^{-3}$ .

In this case, the loss function  $\alpha(\omega)$  can be modeled as

$$\alpha(\omega) = \alpha_0(\omega) - \sum_{j=1}^N \alpha_j(\omega - \omega_j), \quad (1)$$

where  $\alpha_0(\omega)$  is the nonresonant smooth loss profile and  $\alpha_j(\omega - \omega_j)$  is a sharply peaked (centered at  $\omega_j$ ) line shape corresponding to the localized mode  $j$  [ $\alpha_j(\omega)$  is centered at  $\omega = 0$  for later convenience]. Since the RL spectral line is limited, we take  $\alpha_0(\omega) \cong \alpha_0$ . For large systems, we also expect a huge number of modes [9] with comparable properties; we will hence take  $\alpha_j(\omega) \cong \alpha_{\text{avg}}(\omega)$ , where  $\alpha_{\text{avg}}$  is an average resonant line shape. Therefore the oscillation condition becomes

$$\begin{aligned} g[A(\omega)] &= \alpha_0(\omega)A(\omega) - \sum_j \alpha_j(\omega - \omega_j)A(\omega) \\ &\cong \alpha_0 A(\omega) - \sum_j \alpha_{\text{avg}}(\omega - \omega_j)A(\omega_j), \end{aligned} \quad (2)$$

where we exploited the fact that  $\alpha_j(\omega - \omega_j)$  is much narrower than  $A(\omega)$ , and hence it “samples” the emission spectrum at  $\omega_j$ . In the continuum limit, the right-hand side of Eq. (2) becomes

$$\alpha(\omega)A(\omega) \cong \alpha_0 A(\omega) - \int \alpha_{\text{avg}}(\omega - \Omega)A(\Omega)d\Omega. \quad (3)$$

We then consider the left-hand side (amplifying part)  $g[A(\omega)]$  of Eq. (2), and we exploit the passive mode-locking laser theory [38,39]. For a finite gain bandwidth with lifetime  $t_g$ , Eq. (2) in the time domain is

$$g_0 \left[ a(t) + t_g^2 \frac{d^2 a}{dt^2} - \gamma_s |a|^2 a \right] = [\alpha_0 - \phi_L(t)]a, \quad (4)$$

where we introduced the Fourier transform  $a(t)$  of  $A(\omega) = \mathcal{F}[a] = (1/2\pi) \int a(t) \exp(i\omega t) dt$  and  $\phi_L = \mathcal{F}[\alpha_{\text{avg}}]$ . In Eq. (4),  $g_0$  is the small signal gain and  $\gamma_s$  is the gain saturation coefficient [38,39].  $\alpha_{\text{avg}}(\omega)$  is narrow with respect to the gain bandwidth; hence,  $\phi_L(t)$  can be expanded around  $t = 0$ :  $\phi_L(t) \cong (\alpha_0 - \alpha_L)[1 - (t/t_L)^2]$ , where  $\alpha_L$  is the average loss for the high- $Q$  modes ( $\alpha_0 > \alpha_L$ ) and  $t_L$  is their average lifetime. Equation (4) is then cast in a dimensionless form  $a = a_0 \varphi(\tau)$  and  $t = \tau t_0$ , with  $a_0^2 = t_g \sqrt{\alpha_0 - \alpha_L} / \gamma_s \sqrt{g_0} t_L$  and  $t_0^2 = t_g t_L \sqrt{g_0} / \sqrt{\alpha_0 - \alpha_L}$ :

$$-\frac{d^2 \varphi}{d\tau^2} + \tau^2 \varphi + |\varphi|^2 \varphi = E\varphi. \quad (5)$$

The “nonlinear eigenvalue”  $E$  is given by

$$E = \frac{t_L}{t_g} \frac{g_0 - \alpha_L}{\sqrt{(\alpha_0 - \alpha_L)g_0}} = \frac{p - 1}{\kappa \sqrt{p}}, \quad (6)$$

where  $p = g_0/\alpha_L$  is proportional to the pump energy and  $\kappa \equiv (t_g/t_L)(\alpha_0/\alpha_L - 1)^{1/2}$ .

It is known that wave resonances in random systems display a distribution of decay times that is bell-shaped around some value  $t_L$  and with comparable width [40]. Equation (5) is the oscillation condition for these modes with different  $\tau$  (which corresponds to the shift from  $t_L$ ), including gain saturation, finite gain bandwidth, and the mode-coupling due to the overlapping resonances. Equation (5) [or Eq. (4)] is identical to the bound-state GP equation for the 1D Bose-Einstein condensation (BEC) with an external potential  $\phi_L(t)$ . This shows that a spectral region of high- $Q$  modes acts as a trapping potential for the energy levels of the excited photons. Frequencies tend to be concentrated in this spectral range, as Bose-condensed atoms tend to be localized by the external trap [33]. Equation (5) displays bell-shaped solutions for  $E > 1$  (see, e.g., [41]), and this implies a pumping threshold for the laser action; the corresponding dimensionless gain  $p_{\text{th}} = 1 + \kappa^2/2 + \kappa\sqrt{4 + \kappa^2}/2$  is given by  $E = 1$  ( $p_{\text{th}} \cong 1$  as  $\kappa \ll 1$ ). As  $E \geq 1$  ( $p \geq p_{\text{th}}$ ), an approximated solution of Eq. (6) is  $\varphi = 2^{1/4}\sqrt{E-1}\exp(-\tau^2/2)$ . The RL spectrum at the threshold (i.e., for  $p \sim p_{\text{th}}$ ) is hence

$$S(\omega) = |A(\omega)|^2 = \frac{t_g^2}{\sqrt{2\pi}\gamma_S} (E-1) \exp\left[-\frac{\omega^2}{8\pi^2 W_{\text{th}}^2}\right], \quad (7)$$

with the spectral waist (in frequency  $\omega/2\pi$ )

$$2\pi t_g W_{\text{th}} = \sqrt{\frac{\kappa}{2}} = \sqrt{\frac{t_g}{2t_L} \sqrt{\frac{\alpha_0}{\alpha_L} - 1}}. \quad (8)$$

Equation (8) implies that the RL linewidth at threshold is a fraction of the gain bandwidth ( $\sim 1/t_g$ ) given by  $\sqrt{\kappa}/2\sqrt{2}\pi \ll 1$ . For a gain bandwidth of 250 nm and a RL spike linewidth  $\leq 0.5$  nm (i.e.,  $t_L/t_g \cong 500$ ) and taking for the losses  $\alpha_L \cong \alpha_0/1000$  [42], it is  $\kappa \cong 0.1$  and

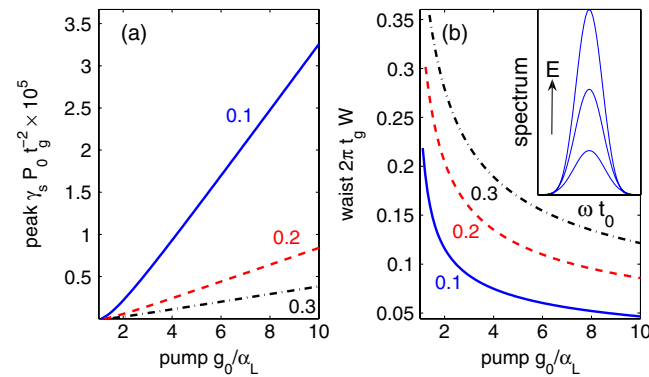


FIG. 3 (color online). Theory: Peak spectrum (a) and spectral waist (b) for various  $\kappa$  versus the pumping rate in dimensionless units. Inset: Spectral profiles for  $E = 1.1, 10$ , and  $20$ .

$2\pi t_g W_{\text{th}} \cong 0.2$ . For  $E > 1$ , the spectral profile is obtained by the numerical solution of (5); from its Fourier transform  $\tilde{\varphi}(\omega t_0)$  [inset in Fig. 3(b)] the normalized waist  $w_\varphi[E(p)]$  and peak  $p_\varphi[E(p)]$  are determined;  $W = w_\varphi\sqrt{\kappa}/p^{1/4}t_g$  and  $S_p = t_g^2 p_\varphi/\gamma_S$  are the corresponding for  $S(\omega)$  in real-world units (Figs. 3 and 5).

In summary, Eq. (6) relates the pumping  $p$  to the non-linear eigenvalue  $E$ , which fixes the spectral line shape through Eq. (4) [or Eq. (5)]; this equation can be hence considered as the equivalent for RL of the ST law.

*Experimental results.*—We use a colloidal dispersion of  $\text{TiO}_2$  (Sachtleben Hombitan R611) particles in methanol doped by Rhodamine B (Sigma-Aldrich R6626); the packing fraction is 0.2 with average index  $\bar{n} = 1.5$  (the measured mean free path by enhanced backscattering for pure methanol is  $\ell = 1700$  nm at  $\lambda = 532$  nm); the RL pump is a 120 ps linearly polarized 10 Hz Nd:Yag laser at 532 nm and 0.8 mm spot size. Emission is retrieved by a fiber coupled spectrograph (Jobin Yvon, focal length 140 mm) and a thermoelectrically cooled CCD camera.

Figure 4 shows the width (standard deviation) and the peak of the spectrum averaged over 100 laser shots versus pump energy  $\mathcal{E}$ ; the RL line first narrows and then stabilizes to a smooth profile. The best fit with the theory (Fig. 5) furnishes  $\kappa \cong 0.14$ ; the threshold pump energy ( $E = 1$ ) is  $\mathcal{E}_{\text{th}} \cong 0.09$  mJ. In Fig. 5(b), we also display the linewidth calculated by a Gaussian fit of the FDTD data (the energy axis has been scaled to fit the experiments).

*Conclusions.*—A theoretical approach based on a non-linear bound-state equation, identical to the GP equation for BEC [33], has been shown to quantitatively agree with experimentally retrieved laser emission in a colloidal dyed-doped dispersion of  $\text{TiO}_2$  particles and with 3D + 1 first-principle numerical simulations. RL emission can be related to a condensation process of several wave resonances in the presence of disorder, the distribution of their decay times playing the role of a temporal trapping potential. The

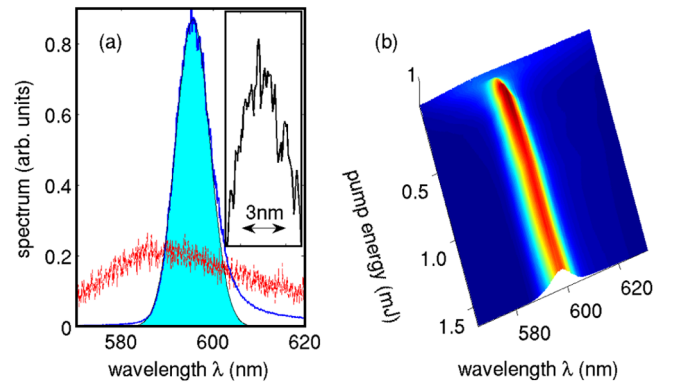


FIG. 4 (color online). Experimental results: (a) spectra at energies 20  $\mu\text{J}$  (thin line) and 1000  $\mu\text{J}$  (shaded area is a Gaussian fit), inset: corresponding enlarged central spectral region; (b) - unitary-area averaged spectra (100 shots) vs energy.

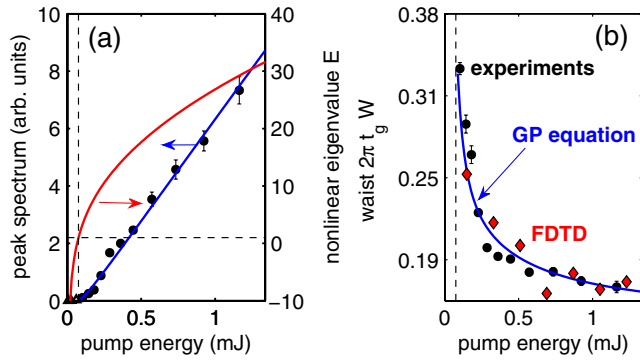


FIG. 5 (color online). (a) Left scale, experimentally retrieved laser peak spectrum versus pump energy, where the line is a best fit from theory; right scale, nonlinear eigenvalue (dashed lines correspond to  $E = 1$ ). (b) Linewidth vs energy; the continuous line is the best fit from theory; the FDTD Maxwell-Bloch simulations (diamonds) are also shown.

simultaneous spectral and temporal narrowing with the number photons in RL is hence corresponding to the spectral and spatial narrowing of the BEC wave function at the condensation.

We acknowledge support from the INFM-CINECA initiative for parallel computing. The research leading to these results has received funding from the European Research Council under the European Community's Seventh Framework Program (FP7/2007-2013)/ERC Grant Agreement No. 201766.

[1] H. Cao, *J. Phys. A* **38**, 10497 (2005).  
 [2] D. S. Wiersma, *Nature Phys.* **4**, 359 (2008).  
 [3] R. Ambartsumyan, N. Basov, P. Kryukov, and S. Lethokov, *IEEE J. Quantum Electron.* **2**, 442 (1966).  
 [4] V. S. Lethokov, *Sov. Phys. JETP* **26**, 835 (1968).  
 [5] N. M. Lawandy, R. M. Balachandran, A. S. L. Gomes, and E. Sauvain, *Nature (London)* **368**, 436 (1994).  
 [6] M. Siddique, Y. Li, and R. R. Alfano, *Opt. Commun.* **117**, 475 (1995).  
 [7] D. Zhang, B. Cheng, J. Yang, Y. Zhang, W. Hu, and Z. Li, *Opt. Commun.* **118**, 462 (1995).  
 [8] R. C. Polson and Z. V. Vardeny, *Appl. Phys. Lett.* **85**, 1289 (2004).  
 [9] K. L. van der Molen, A. P. Mosk, and A. Lagendijk, *Phys. Rev. A* **74**, 053808 (2006).  
 [10] S. Mujumdar, V. Turck, R. Torre, and D. S. Wiersma, *Phys. Rev. A* **76**, 033807 (2007).  
 [11] A. Yariv, *Quantum Electronics* (Saunders College, San Diego, 1991).  
 [12] A. L. Schawlow and C. H. Townes, *Phys. Rev.* **112**, 1940 (1958).  
 [13] C. W. J. Beenakker, *Phys. Rev. Lett.* **81**, 1829 (1998).

[14] M. Patra, *Phys. Rev. A* **65**, 043809 (2002).  
 [15] G. Hackenbroich, C. Viviescas, B. Elattari, and F. Haake, *Phys. Rev. Lett.* **86**, 5262 (2001).  
 [16] H. Cao, *Waves Random Complex Media* **13**, R1 (2003).  
 [17] L. Angelani, C. Conti, G. Ruocco, and F. Zamponi, *Phys. Rev. Lett.* **96**, 065702 (2006).  
 [18] D. S. Wiersma and A. Lagendijk, *Phys. Rev. E* **54**, 4256 (1996).  
 [19] S. John and G. Pang, *Phys. Rev. A* **54**, 3642 (1996).  
 [20] L. Florescu and S. John, *Phys. Rev. E* **70**, 036607 (2004).  
 [21] A. Lubatsch, J. Kroha, and K. Busch, *Phys. Rev. B* **71**, 184201 (2005).  
 [22] L. I. Deych, *Phys. Rev. Lett.* **95**, 043902 (2005).  
 [23] H. E. Tureci, L. Ge, S. Rotter, and A. D. Stone, *Science* **320**, 643 (2008).  
 [24] C. Gouedard, D. Husson, C. Sauteret, F. Auzel, and A. Migus, *J. Opt. Soc. Am. B* **10**, 2358 (1993).  
 [25] M. Siddique, R. R. Alfano, G. A. Berger, M. Kempe, and A. Z. Genack, *Opt. Lett.* **21**, 450 (1996).  
 [26] V. M. Papadakis, A. Stassinopoulos, D. Anglos, S. H. Anastasiadis, E. P. Giannelis, and Papazoglou, *J. Opt. Soc. Am. B* **24**, 31 (2007).  
 [27] X. Jiang and C. M. Soukoulis, *Phys. Rev. Lett.* **85**, 70 (2000).  
 [28] P. Sebbah and C. Vanneste, *Phys. Rev. B* **66**, 144202 (2002).  
 [29] *Scattering and Localization of Classical Waves in Random Media*, edited by P. Sheng (World Scientific, Singapore, 1990).  
 [30] R. M. Balachandran, N. M. Lawandy, and J. A. Moon, *Opt. Lett.* **22**, 319 (1997).  
 [31] G. A. Berger, M. Kempe, and A. Z. Genack, *Phys. Rev. E* **56**, 6118 (1997).  
 [32] S. Mujumdar, M. Ricci, R. Torre, and D. S. Wiersma, *Phys. Rev. Lett.* **93**, 053903 (2004).  
 [33] F. Dalfovo, S. Giorgini, L. P. Pitaevskii, and S. Stringari, *Rev. Mod. Phys.* **71**, 463 (1999).  
 [34] C. Connaughton, C. Josserand, A. Picozzi, Y. Pomeau, and S. Rica, *Phys. Rev. Lett.* **95**, 263901 (2005).  
 [35] A. Fratolocci, C. Conti, and G. Ruocco, *Opt. Express* **16**, 8342 (2008); *Phys. Rev. A* **78**, 013806 (2008).  
 [36] C. Conti and A. Fratolocci, arXiv:0802.3775v1 [Nature Phys. (in press)].  
 [37] C. Conti, L. Angelani, and G. Ruocco, *Phys. Rev. A* **75**, 033812 (2007).  
 [38] H. A. Haus, *IEEE J. Sel. Top. Quantum Electron.* **6**, 1173 (2000).  
 [39] J. N. Kutz, *SIAM Rev.* **48**, 629 (2006).  
 [40] A. A. Chabanov, Z. Q. Zhang, and A. Z. Genack, *Phys. Rev. Lett.* **90**, 203903 (2003).  
 [41] Y. S. Kivshar, T. J. Alexander, and S. K. Turitsyn, *Phys. Lett. A* **278**, 225 (2001).  
 [42]  $1/\alpha_0$  is taken as the time needed to travel a mean free path  $\ell$  at velocity  $c/\bar{n}$ ; with  $\bar{n} = 1.5$  and  $\ell \cong 1700$  nm ( $k\ell \cong 20$ ), one finds  $1/\alpha_0 \cong 10$  fs, assuming  $1/\alpha_L \cong 2t_L \cong 10$  ps (i.e.,  $\alpha_0/\alpha_L \cong 1000$ ).